Science and Technology of Advanced Materials

ISSN: 1468-6996 (Print) 1878-5514 (Online) Journal homepage: https://www.tandfonline.com/loi/tsta20

Classification of silica fine particles using a novel electric hydrocyclone

Wongsarivej Pratarn, Tanthapanichakoon Wiwut & Hideto Yoshida

To cite this article: Wongsarivej Pratarn, Tanthapanichakoon Wiwut & Hideto Yoshida (2005) Classification of silica fine particles using a novel electric hydrocyclone, Science and Technology of Advanced Materials, 6:3-4, 364-369, DOI: 10.1016/j.stam.2005.02.015

To link to this article: https://doi.org/10.1016/j.stam.2005.02.015

Published online: 20 Jun 2005.

ELSEVIER

Science and Technology of Advanced Materials 6 (2005) 364–369

SCIENCE AND TECHNOLOGY OF ADVANCED MATERIALS

www.elsevier.com/locate/stam

Classification of silica fine particles using a novel electric hydrocyclone

Wongsarivej Pratarn[a], Tanthapanichakoon Wiwut[b,*], Hideto Yoshida[c]

[a]*Department of Chemical Engineering, Faculty of Engineering, Chulalongkorn University, Bangkok 10330, Thailand*
[b]*National Nanotechnology Center, Thailand Science Park, 111 Paholyothin Road, Klong Luang, Pathumthani 12120, Thailand*
[c]*Department of Chemical Engineering, Faculty of Engineering, Hiroshima University, Hiroshima, Japan*

Received 12 January 2005; revised 15 February 2005; accepted 15 February 2005
Available online 20 June 2005

Abstract

A novel electric hydrocyclone is developed and tested. Aqueous suspensions of silica with a median diameter of 754 nm and 0.2% volumetric concentration are tested using a 20-mm-diameter hydrocyclone. The ratios of tested underflow rate to throughput are: 0, 0.1, 0.2 and 0.3. The tested volumetric flow rates are 0.083×10^{-3}, 0.117×10^{-3} and 0.167×10^{-3} m^3/s (5, 7 and 10 l/min). The conical part of the electric hydrocyclone is connected to a cylindrical dust box having 42 mm diameter. This dust box has a central metal rod cone and a cylindrical metal wall between which the desired 50-volt DC electric potential or no potential is applied. The investigated lengths of the dust box are 53 and 106 mm. The three different conditions investigated are: (a) no applied electric potential, (b) positive potential applied at the central rod side and negative potential at the side wall, and (c) positive potential applied at the side wall and negative potential at the central rod side. In both the absence and presence of the underflow, the hydrocyclone with a long dust box is found to give better classification efficiency than that with a short dust box. Interestingly, the effect of electric potential is reversed with respect to the presence and absence of the underflow. The presence of the underflow unexpectedly increase the 50% particle cut size when electric potential is applied. However, the effect of electric potential is reversed when there is no underflow. The electric potential can reduce the 50% particle cut size by up to 10% compared to the absence of electricity. It is found that condition (c) exhibits a stronger effect than condition (b). As expected, the higher the flow ratio, the smaller the particle cut size becomes. Based on the experimental results, an empirical correlation for the 50% particle cut size has been obtained.

Keywords: Classification; Silica; Particles; Electric; Hydrocyclone

1. Introduction

Silica is a hard abrasive mineral used in numerous industries. Grinding is a common important process to produce silica fine particles. In the dry grinding process, fugitive dust is easily created. When people inhale the fine dust of crystalline silica, it can lead to silicosis, a potentially fatal lung disease. Wet grinding not only eliminates fugitive dust but also gives higher grinding efficiency. The coarse oversize particles have to be separated out and sent back for regrinding. The conventional hydrocyclone is suitable for the classification of relatively fine, though not too fine, particles unclassifiable by sifting.

A hydrocyclone [1,2] is simple in construction, has no moving parts, requires low installation and maintenance investment for the separation, classification and thickening in many solid–liquid processes. Though originally designed to promote solid–liquid separations, they are also used for solid-solid [3], liquid–liquid [4], and gas–liquid separation [5]. Although the first patent on a hydrocyclone is about 115 years old, research works are still in progress aiming at developing new applications [6–10] or understanding the complex phenomena inside it.

Two well-known theories for particle separation in hydrocyclones are the equilibrium orbit theory [11] and the residence time theory [12]. The former assumes that particles of a given size will reach an equilibrium radial orbit position inside the hydrocyclone where their outward terminal settling velocity is equal to the inward radial velocity of the liquid. Accordingly to this theory, larger

* Corresponding author. W. Tanthapanichakoon Tel.: +66 2 564 7123; fax: +66 2 564 7122.
E-mail address: wiwut@nanotec.or.th (T. Wiwut).

1468-6996/$ - see front matter © 2005 Elsevier Ltd. All rights reserved.
doi:10.1016/j.stam.2005.02.015

Nomenclature

d_{50}	50% Particle cut size (μm)	L	Total length of hydrocyclone (m)
D_c	Hydrocyclone body diameter (m)	Q	Suspension feed flow rate (m^3/s)
D_i	Inlet diameter (m)	R_f	Underflow to throughput ratio (flow ratio) (−)
D_o	Overflow diameter (m)	μ	Viscosity of suspension (kg/ms)
D_u	Underflow diameter (m)	ρ	Density of water (kg/m^3)
G	Grade efficiency (−)	ρ_p	Density of silica particle (kg/m^3)
l	Vortex finder length (m)		

particles will attain a radial orbit position near the wall, where the axial fluid velocity has a downward direction. These particles will leave the cyclone through the underflow. The radial orbit position of smaller particles will be located near the center, inside the region where the axial fluid velocity is upward. These particles will escape through the overflow. The cut size is defined as the particle size whose equilibrium orbit is coincident with the locus of zero vertical velocity of the fluid. Such a particle will have equal chances to escape the hydrocyclone either through the underflow or through the overflow. According to the residence time theory, a particle will be separated as a function of both the position it enters the cyclone and the available residence time. The cut size will be the size of the particle which entering the equipment exactly in the center of the inlet pipe will just reach the wall in the residence time available. Several authors have used either theory to derive different equations for predicting the cut size [13–16].

The study of size classification performance, in terms of both fundamental and operational variables has been undertaken by several authors [17–20]. Empirical models have been developed [18–21] which are used for predicting hydrocyclone performance in terms of capacity, cut size and water split. With respect to the empirical modeling of small diameter hydrocyclones, some studies [22–24] describe hydrocyclone performance with new correlations for the capacity, cut size and water split. The flow pattern in hydrocyclones has been examined experimentally [18,23, 25] and theoretically [12,18,26]. Expressions for d_{50} have been obtained empirically [27–30] and theoretically [31,32]. The purpose of this study is to verify the collection efficiency of a new type of electric hydrocyclone with and without underflow under applied electric potential at the dust box. The simple correlation for the 50% cut size is discussed.

2. Materials and methods

Silica is used as the test powder which has the particle size distribution as shown in Fig. 1. The median diameter is 754 nm. The density of powder is 2210 kg/m^3. Deionised water is used in all experiments. Suspensions of 0.2% solid content by weight are tested in hydrocyclone of 20 mm body diameter. All design proportions are as shown in Table 1.

The ratios of tested underflow rate to throughput are: 0, 0.1, 0.2 and 0.3. The tested volumetric flow rates are 0.083×10^{-3}, 0.117×10^{-3} and 0.167×10^{-3} m^3/s. The operating time is 20 min to assure that the system is in steady state.

The simplified experimental apparatus is shown in Fig. 2. As can be seen, it consists of a tank equipped with impeller for mixing at constant speed of 250 rpm. The discharged underflow and overflow are returned to the feed tank. The flow meter and pressure gauge are installed to measure flow rate and pressure drop. The suspension temperature in the tank is constantly controlled at 30 °C by using cooler and heater.

The conical part of the electric hydrocyclone is connected to a cylindrical dust box having 42 mm diameter. This dust box has a central metal rod cone and a cylindrical metal wall between which the desired 50-volt DC electric potential or no potential is applied. The investigated lengths of the dust box are 53 and 106 mm. The three different conditions investigated are: (a) no applied electric potential, (b) positive potential applied at the central rod side and

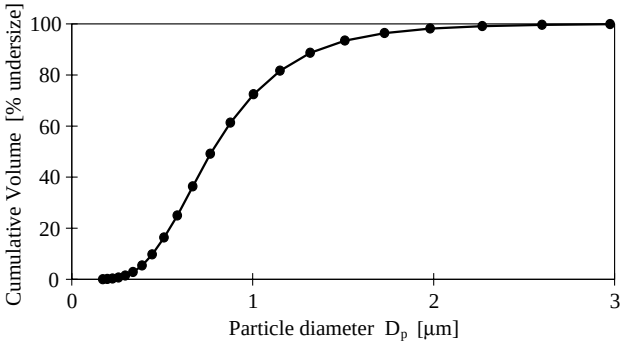

Fig. 1. Particle size distribution of the feed materials.

Table 1
Hydrocyclone proportions

D_i/D_c	D_o/D_c	D_u/D_c	l/D_c	L/D_c	Cone angle (°)
0.20	0.16	0.20	1.00	7.40	7.68

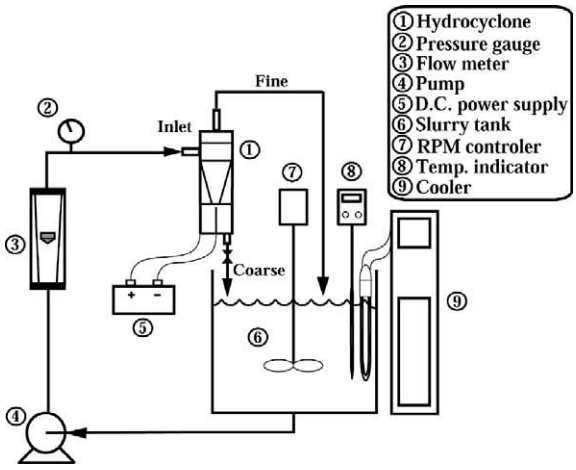

Fig. 2. Experimental apparatus.

negative potential at the side wall, and (c) positive potential applied at the side wall and negative potential at the central rod side.

The particle size analyses of both effluent streams are carried out by Laser Scattering Particle Size Distribution Analyser, HORIBA LA-920 with $(NaPO_3)_6$ 0.3 g as a dispersing agent. The concentrations of solids in the underflow and overflow samples are measured by evaporation and weighing. The grade efficiency, G, and the cut size, d_{50}, are evaluated according to the procedure recommended by Svarovsky [2].

3. Results and discussion

Fig. 3 shows the effect of dust box length in the absence of the underflow. The hydrocyclone with a longer dust box exhibits higher separation efficiency because coarse particles have less chance to escape from the vortex finder than that with a short one. At steady state, the 50% cut size are 2.260 and 1.858 μm for the short dust box at flow rate 0.117×10^{-3} and 0.167×10^{-3} m^3/s, respectively but

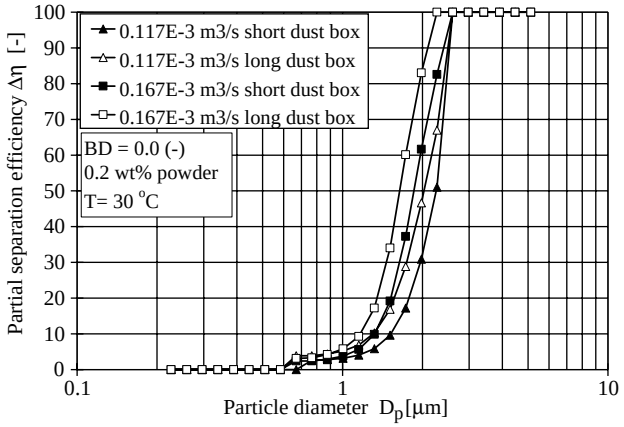

Fig. 3. Effect of dust box length in the absence of underflow.

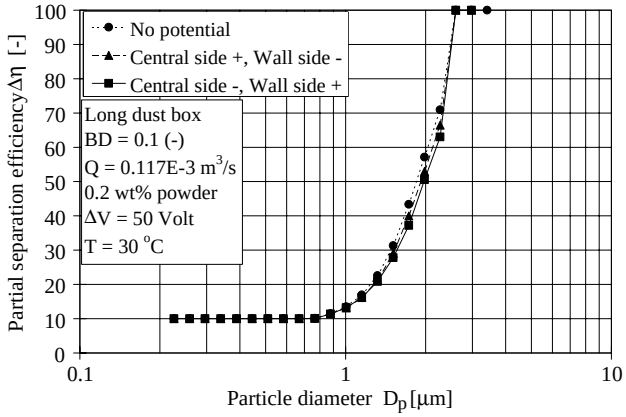

Fig. 4. Effect of potential in the presence of underflow.

decreases by 10.22% to 2.029 μm and by 11.52% to 1.644 μm for the long dust box.

Figs. 4 and 5 show the particle separation efficiency when electric potential is applied to the long dust box of the hydrocyclone in the presence and absence of the underflow, respectively. The effect of electric potential is reversed with respect to the presence and absence of the underflow. More specifically, the electric potential for positive pole at both the central rod and side wall increases the 50% particle cut size when compared with no application of electric potential in the presence of the underflow. The trend is reversed in the absence of the underflow. Both in the absence and presence of the underflow, effect of the potential when the positive pole is connected to the side wall is stronger than when the positive pole is connected to the central rod.

Fig. 6 shows the relationship between 50% particle cut size, d_{50}, and the underflow to throughput ratio, R_f, by using the long dust box at feed flow rate 0.117×10^{-3} m^3/s with and without electric potential. As expected, the higher the flow ratio, the smaller the particle cut size becomes. The choice is between high flow ratios at low-pressure drops, or low flow ratios at high-pressure drops. However,

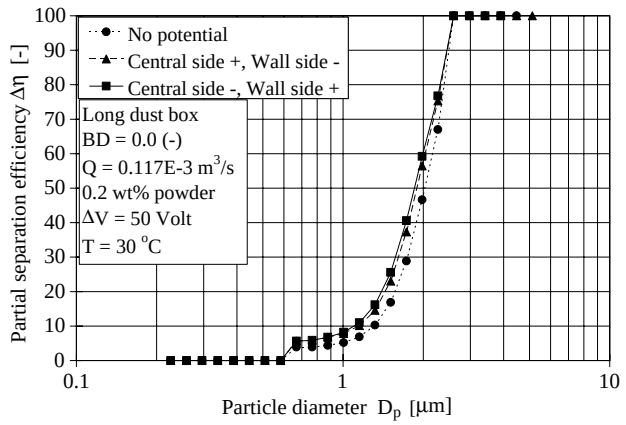

Fig. 5. Effect of potential in the absence of underflow.

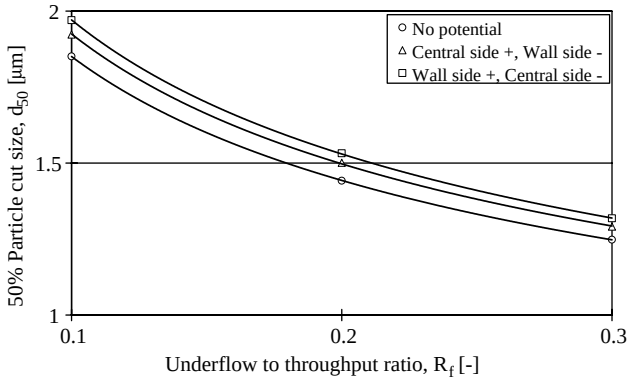

Fig. 6. Relationship between d_{50} and R_f using the long dust box.

a higher flow ratio results in a lower solid concentration and vice versa. Depending on the particle size of the feed solids and the cost of further dewatering of the solids in the underflow, the two running costs of dewatering of the solids in the underflow and pressure drop should be weighed against each other and the operating conditions optimized accordingly.

Fig. 7 shows the relationship between d_{50} and suspension feed flow rate, Q, for either the short or long dust box at operating flow ratio 0.1 with and without electric potential. As anticipated, the higher the feed flow rate, the smaller the particle cut size. The results confirm both the effect of dust box length in Fig. 3 and trend of electric potential effects in Figs. 4 and 6. Similarly, Fig. 8 shows the relationship between d_{50} and Q for short or long dust boxes with no underflow in the absence and presence of electric potential. The higher feed flow rate reduces the smaller particle cut size. The results again confirm both effects of dust box length in Fig. 3 and trend of electric potential in Fig. 5. In order to obtain the smallest cut size the long dust box should be selected and the system operated with positive electric potential at the wall and no underflow.

Fig. 9 shows the correlation results for the d_{50} in the presence and absence of underflow using parameters K_1,

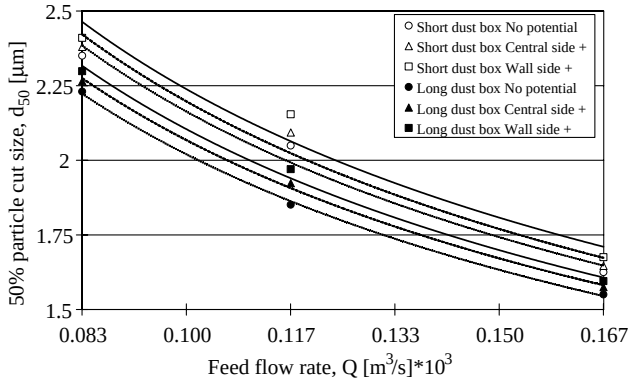

Fig. 7. Relationship between d_{50} and Q at flow ratio 0.1.

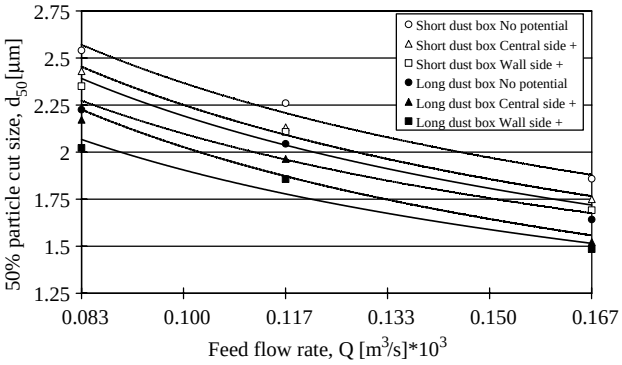

Fig. 8. Relationship between d_{50} and Q with no underflow.

C_1 and C_2 (see Appendix A) compared with experimental results in the presence and absence of underflow, respectively. The estimated parameters are agreed well with experimental results.

4. Conclusion

In both the absence and presence of the underflow, the hydrocyclone with a long dust box is found to give better classification efficiency than that with a short dust box. Interestingly, the effect of electric potential is reversed with respect to the presence and absence of the underflow. The presence of the underflow unexpectedly increase the 50% particle cut size when electric potential is applied. However, the effect of electric potential is reversed when there is no underflow. The electric potential can reduce the 50% particle cut size by up to 10% compared to the absence of electricity. It is found that condition (c) with positive potential applied at the side wall and negative potential at the central rod side exhibits a stronger effect than condition (b) with positive potential applied at the central rod side and negative potential at the side wall. As expected, the higher the flow ratio, the smaller the particle

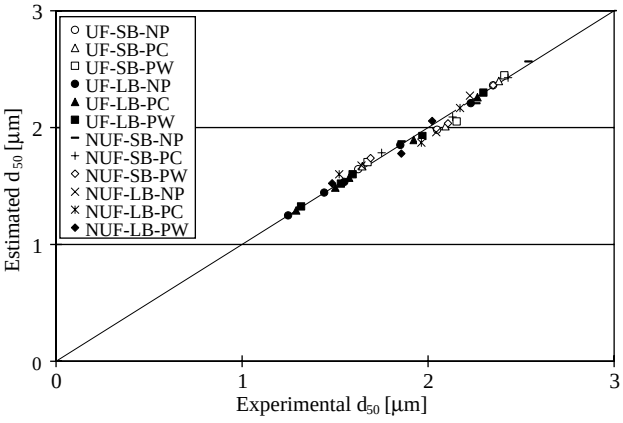

Fig. 9. Correlation results for the d_{50} in the presence and absence of underflow (UF, underflow; NUF, no underflow; SB, short box; LB, long box; NP, no potential; PC, positive center; PW, positive wall).

Table A1
The constants for the presence and absence of the underflow in Eq. (A.4)

		C_1	C_2		
			No	Center+	Wall+
Presence of underflow	Short dust box	3067	0	744	1698
	Long dust box	0	0	1036	1815
Absence of underflow	Short dust box	5836	0	−2759	−4045
	Long dust box	0	0	−2114	−4323

cut size becomes. Based on the experimental results, an empirical correlation for the 50% particle cut size has been obtained as Eqs. (A.3)–(A.6).

Acknowledgements

P.W. acknowledged Royal Golden Jubilee PhD scholarship from Thailand Research Fund (TRF), 1-year Student Exchange Scholarship from Association of International Education Japan and useful comments from Dr Kunihiro Fukui, Hiroshima University. This work was partially supported by Thailand–Japan Technology Transfer Project and TRF-RTA Project of Prof. Wiwut Tanthapanichakoon.

Appendix A

The correlation derived from equation of motion is

$$m\frac{\mathrm{d}u_\mathrm{r}}{\mathrm{d}t} = -3\pi\mu D_\mathrm{p}(u_\mathrm{r} - v_\mathrm{r}) + \frac{mv_\theta^2}{r} \tag{A.1}$$

where u and v are particle and fluid velocity that respect to coordinate, respectively. At steady state the left hand term is zero, so that:

$$D_\mathrm{p} = \sqrt{\frac{18\ \mu r(u_\mathrm{r} - v_\mathrm{r})}{(\rho_\mathrm{p} - \rho)v_\theta^2}}$$

At critical particle velocity, $u_\mathrm{r}=0$:

$$D_\mathrm{pc} = \left(\frac{18\ \mu r(-v_\mathrm{r})}{\rho_\mathrm{p} - \rho)v_\theta^2}\right)^{1/2} = \left(\frac{18\ \mu r(v_\mathrm{R})}{(\rho_\mathrm{p} - \rho)v_\theta^2}\right)^{1/2}$$

Normally, $v_\theta = v_i$, $v_\mathrm{R} = \alpha v_\mathrm{i}, v_i = 4Q/\Pi D_i^2$ and $r = D_\mathrm{c}/2$

$$D_\mathrm{pc} = (7.07\alpha)^{1/2}\left(\frac{\mu D_\mathrm{c}D_\mathrm{i}^2}{(\rho_\mathrm{p} - \rho)Q}\right)^{1/2}$$

$$= K\left(\frac{\mu D_\mathrm{c}D_\mathrm{i}^2}{(\rho_\mathrm{p} - \rho)Q}\right)^{1/2} \tag{A.2}$$

Substitute with the cyclone dimensions and property:

$$d_{50} = K\left(\frac{0.8328\times10^{-3}\times20\times10^{-3}\times(3.9\times10^{-3})^2}{(2210 - 995.647)Q}\right)^{0.5}$$

$$d_{50} = K\left(\frac{2.0862\times10^{-13}}{Q}\right)^{0.5} \tag{A.3}$$

The semi-empirical constant K is denoted by:

$$K = K_1 + C_1 + C_2 \tag{A.4}$$

where K_1 is a constant. C_1 and C_2 denote the dust box length effect and electric effect respectively. The correlation for the presence of the underflow is:

$$K_1 = \frac{15338}{Q^{0.0245}R_f^{0.359}} \tag{A.5}$$

The correlation for the absence of the underflow is:

$$K_1 = 79746Q^{0.0599} \tag{A.6}$$

The constants for the presence and absence of the underflow in Eq. (A.4) are shown in Table A1.

References

[1] D. Bradley, The Hydrocyclone, Pergamon, London, 1965, p. 1.
[2] L. Svarovsky, Solid–Liquid Separation, Butterworth, New York, 1981, p. 202.
[3] M.S. Klima, B.H. Kim, Dense-medium separation of heavy-metal particles from soil using a wide-angle hydrocyclone, J. Environ. Sci. Health., Part A 33 (1998) 1325–1340.
[4] C.A. Capela Moraes, C.M. Hackenberg, C. Russo, R.A. Medronho, Theoretical analysis of oily water hydrocyclones, in: D. Claxton, L. Svarovsky, M. Thew (Eds.), Hydrocyclones'96, Mechanical Engineering Publications, London and Bury Saint Edmunds, 1996, pp. 383–398.
[5] S. Marti, Analysis of gas carry-under in gas–liquid cylindrical cyclones, in: D. Claxton, L. Svarovsky, M. Thew (Eds.), Hydrocyclones'96, Mechanical Engineering Publications, London and Bury Saint Edmunds, 1996, pp. 399–421.
[6] V.M. Matta, R.A. Medronho, A new method for yeast recovery in batch ethanol fermentations: filter aid filtration followed by separation of yeast from filter aid using hydrocyclones, Bioseparation 9 (2000) 43–53.
[7] M. Lubberstedt, R.A. Medronho, F.B. Anspach, W.D. Deckwer, Separation of mammalian cells using hydrocyclones, in: Proceedings of the World Congress on Biotechnology—Biotechnology 2000, Berlin, vol. 1, 2000, pp. 460–462.

[8] M. Lubberstedt, R.A. Medronho, F.B. Anspach, W.D. Deckwer, Abtrennung tierischer Zellen mot Hydrozyklonen, Chem. Ing. Technol. 72 (2000) 1089–1090.
[9] J.J. Cilliers, S.T.L. Harrison, The application of mini-hydrocyclones in the concentration of yeast suspensions, Chem. Eng. J. 65 (1997) 21–26.
[10] H. Yaun, D. Rickwood, I.C. Smyth, M.T. Thew, An investigation into the possible use of hydrocyclones for the removal of yeast from beer, Bioseparation 6 (1996) 159–163.
[11] M.G. Driessen, Theory of flow in a cyclone, Rev. L'Industrie Min. spl. (1951) 449–461.
[12] K. Rietema, Performance and design of hydrocyclones. Parts I–IV, Chem. Eng. Sci. 15 (1961) 298–325.
[13] L. Svarovsky, Hydrocyclones, Holt, Rinehart and Winston, London, 1984.
[14] R.A. Medronho, Scale-up of hydrocyclones at low feed concentrations, PhD Thesis, University of Bradford, Bradford, UK, 1984.
[15] R.A. Medronho, L. Svarovsky, Tests to verify hydrocyclone scale-up procedure, in: Proceedings of the Second International Conference on Hydrocyclones, BHRA, Bath, UK, 1984, pp. 1–14.
[16] M. Antunes, R.A. Medronho, Bradley hydrocyclones: design and performance analysis, in: L. Svarovsky, M.T. Thew (Eds.), Hydrocyclones: Analysis and Applications, Kluwer, Dordrecht, 1992, pp. 3–13.
[17] D.A. Dahlstrom, Cyclones operating factors and capacities on coal and refuse slurries, Mining Trans. 184 (1949) 331–422.
[18] N. Yoshioka, Y. Hotta, Liquid cyclones as a hydraulic classifier, Chem. Eng. Jpn 19 (12) (1959) 632–640.
[19] A.J. Lynch, T.C. Rao, Modeling and scale-up of hydrocyclone classifiers, in: Proceedings of the 11th International Mineral Processing Congress, Cagliari, 1975.
[20] R. Plitt, Mathematical model of the hydrocyclone classifier, CIM Bulletin (1976) 114–123.
[21] A.J. Lynch, in: D.W. Fuerstenau (Ed.), Mineral Crushing and Grinding Circuits, vol. 1 (1977).
[22] G. Rouse, et al., Confirmation of modeling techniques for small diameter cyclones, in: P. Wood, et al. (Ed.), Third International Conference on Hydrocyclones, BHRA, Session A, 1987.
[23] D. Bradley, D. Pulling, Flow patterns in the hydraulic cyclone and their interpretation in terms of performance, Trans. Inst. Chem. Eng. (1959) 37.
[24] G. Brookes, et al., Hydrocyclones performance related to velocity parameters, in: Second International Conference on Hydrocyclones, BHRA, Session C, 1984.
[25] D.F. Kelsall, A study of motion of solid particles in a hydraulic cyclone, Trans. Inst. Chem. Eng. 30 (1952) 87.
[26] F.J. Fontein, C. Dijksman, Recent Developments in Mineral Dressing, Institution of Mining and Metallurgy, London, 1953, p. 229.
[27] D.A. Dahlstrom, Chem. Eng. Prog. Symp. Ser. No. 15 (1954) 50, 41.
[28] B. Elcox, Trans. Corn. Inst. Min. Mech. Metall. Engrs 9 (1953) 26.
[29] P.A. Haas, et al., Chem. Eng. Prog. 53 (1957) 203.
[30] I.R.M Chaston, Trans. Inst. Mining Met. 67 (1958) 203.
[31] A.L. De Gelder, Scaling-up of Chemical Plant and Processes, Institution of Chemical Engineers, London, 1957, p. S47.
[32] H. Trawinski, Chemie-Ingr-Tech. 30 (1958) 85.